Wavelength Reuse in the WDM Optical Interface of a Millimeter-Wave Fiber-Wireless Antenna Base Station

Ampalavanapillai Nirmalathas, *Member, IEEE*, Dalma Novak, *Senior Member, IEEE*, Christina Lim, *Member, IEEE*, and Rodney B. Waterhouse, *Member, IEEE*

***Abstract*—A novel technique for wavelength reuse has been proposed to simplify the upstream optical interface of an antenna base station in a millimeter-wave fiber-wireless system incorporating wavelength division multiplexing. This technique is based on recovering the optical carrier used in downstream signal transmission and reusing the same wavelength for upstream signal transmission. Two novel configurations for optical carrier recovery and wavelength reuse are proposed and demonstrated experimentally.**

***Index Terms*—Fixed wireless access networks, millimeter-wave communications, optical communications.**

I. Introduction

FOR FUTURE provision of broad-band, interactive services over the wireless media, millimeter-wave frequencies have been considered worldwide [1]. In such broad-band wireless access networks, multiple antenna base stations (BSs) provide the wireless connectivity to users via millimeter-wave radio links and the antenna BSs are networked with a central office (CO), which performs the switching and routing functionality. Due to higher radio propagation losses at millimeter-wave frequencies, coverage areas of antenna BSs are small, leading to pico- or micro-cellular wireless network architectures. In addition, small coverage areas in conjunction with high propagation losses provide a unique advantage in managing scarce radio bandwidth by utilizing efficient frequency reuse and by deploying sectorization of the BS antenna's coverage area. However, this leads to an increase in the number of antenna BSs in an area and the provision of broad-band communications between multiple antenna BSs and the CO becomes a challenge.

Optical fibers, due to their obvious advantages in terms of low loss, high immunity to electromagnetic interference, and, most importantly, wide bandwidth characteristics, can be deployed to provide the broad-band interconnection of multiple remote antenna BSs with the CO [2], [3]. In addition, scaleable and easy-to-manage fiberfeed networks can be easily realized by incorporating wavelength division multiplexing (WDM) technologies [4]–[6]. In such millimeter-wave fiber-wireless systems, BSs with simplified RF interfaces can be realized if the radio signals are distributed over fiber at millimeter-wave frequencies ("RF-over-fiber" signal transport), as they require no up- or down-frequency conversion at the BSs.

To support the full-duplex operation of fiber-wireless networks, the optical interfaces of the BSs must include optical sources, which can be modulated by the millimeter-wave uplink radio signals. However, when an optical carrier with millimeter-wave modulation sidebands is transported over fiber, chromatic dispersion can cause RF power penalties [7], [8] as well as a degradation in the detected RF carrier phase noise due to optical decorrelation [9]. Optical single sideband with carrier (OSSB+C) modulation can be used to suppress such RF power penalties [10]. To reduce the phase-noise degradation, however, optical sources with narrow linewidths at well-specified wavelengths are required at the BSs in fiber-wireless systems [9]. Unfortunately, this scenario is not an attractive option for upstream signal transmission as low-cost, ultrastable, narrow-linewidth WDM wavelength lasers are difficult to realize. Therefore, there is a significant advantage in not requiring a wavelength source at the BS, as wavelength assignment and source monitoring can be done at the CO if active sources are only located there.

BSs without any optical sources were first proposed and demonstrated as part of British Telecom's passive pico-cell concept [11] where an electroabsorption modulator (EAM) was used as a detector and modulator by careful choice of an appropriate biasing condition [12]. In this technique, the efficiency of the up- and downstream links were optimized independently via the use of two optical signals at different wavelengths (one for downstream transmission and the other for upstream), so that the EAM was optimized independently for detection and modulation [13]. However, such an approach increases the number of wavelengths required in the system.

In order to avoid the requirement for a high-quality optical source at the BS of a millimeter-wave fiber-wireless systems, we have previously proposed a technique by which a portion of the downstream wavelength signal can be recovered and reused for upstream signal transmission [14]. Subsequently, we proposed and demonstrated two novel configurations for recovery of the optical carrier at the antenna BS [15]. In this paper, we extend the investigation of the optical recovery configurations to consider an experimental demonstration of bi-directional signal transmission of a 155-Mb/s psuedorandom data stream using binary phase-shift keying (BPSK) modulation of the millimeter-wave carriers.

Manuscript received January 14, 2001; revised May 29, 2001.

A. Nirmalathas, D. Novak, and C. Lim are with the Australian Photonics Cooperative Research Centre, Photonics Research Laboratory, Department of Electrical and Electronic Engineering, The University of Melbourne, Melbourne, Vic. 3010, Australia (e-mail: a.nirmalathas@ieee.org).

R. B. Waterhouse is with the Australian Photonics Cooperative Research Centre, School of Electrical and Comupter Systems Engineering, RMIT University, Melbourne, Melbourne, Vic. 3000, Australia.

Publisher Item Identifier S 0018-9480(01)08723-3.

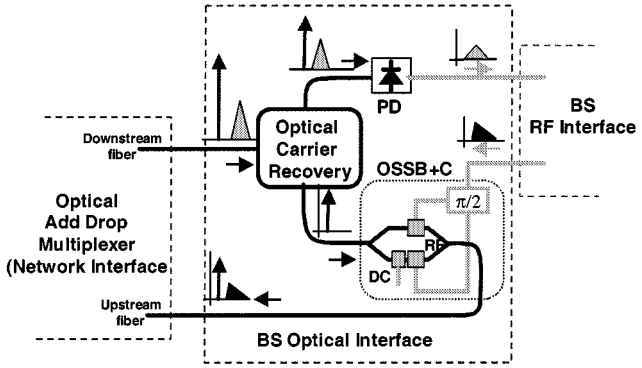

Fig. 1. Simplified optical interface of a fiber-wireless BS using optical carrier recovery.

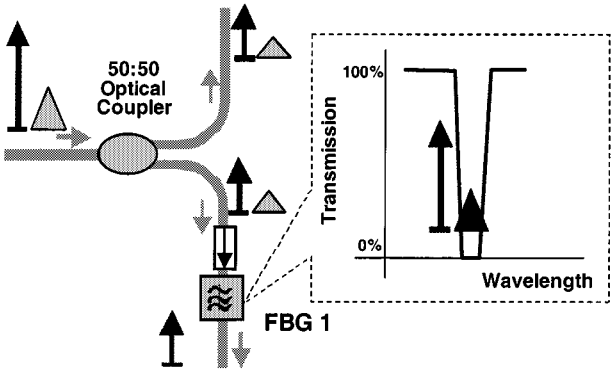

Fig. 2. Configuration A for optical carrier recovery based on an optical coupler in conjunction with an FBG filter.

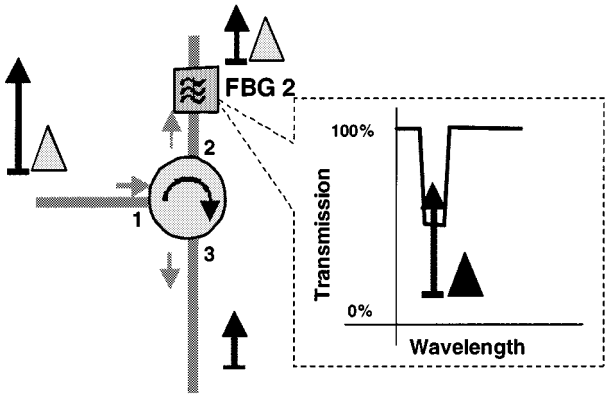

Fig. 3. Configuration B for optical carrier recovery based on an optical circulator in conjunction with an FBG filter.

The paper is organized as follows. Section II describes the WDM optical interface of an antenna BS, which incorporates the proposed optical carrier recovery technique and OSSB+C modulation. In Section III, two configurations for optical carrier recovery using optical fiber Bragg grating (FBG) filters are outlined. Section IV then describes the experimental setup used to demonstrate the operation of the optical carrier recovery configurations in bi-directional RF-over-fiber transmission with experimental results presented in Section V. Finally, the conclusions of this work are summarized in Section VI.

II. Simplified Optical Interfaces of BSs

Fig. 1 shows the proposed optical interface of an antenna BS with interconnections to the optical network interface as well as the RF interface of the BS. In a network incorporating WDM, the BS will be connected to the network via an optical add–drop multiplexer (OADM). The network topology can be either tree, ring, or bus type and the location of the OADM can be in a different location (Remote Node) or at the BS itself depending on the network rollout plan. In such a network, one wavelength can be assigned to the BS, which will use the assigned wavelength for both downstream (transmission from the CO to the BS) and upstream transmission (BS to the CO).

The downstream optical signal destined for the given BS is selected by an OADM, which then directs that signal to the BS downstream optical fiber. By incorporating an optical recovery technique, the need for a WDM optical source with very low phase-noise and RIN specifications for upstream transmission is avoided. This is achieved by extracting part of the downstream optical signal comprising the wavelength carrier and a single modulation sideband (as shown in Fig. 1) and recovering the optical carrier via an optical recovery technique. The other portion of the downstream optical signal is detected by a photodetector (PD), which is then applied to the downstream RF interface of the BS for transmission over the radio link. By reusing the same wavelength in both directions, scarce wavelength resources can be efficiently allocated. In addition, if high-power sources are available, a number of network segments connected to the central office via separate fiber plants can share the same optical sources.

To support dispersion-tolerant RF-over-fiber signal transport, it is assumed that OSSB+C modulation is used in both up- and down-stream directions. As shown in Fig. 1, OSSB+C modulation is realized by using a dual-electrode Mach–Zhender modulator (DE-MZM) in conjunction with an RF hybrid coupler. The upstream electrical signal obtained from the BS RF interface, after being transmitted over the radio link, is split into equal parts but with a phase difference of $\pi/2$ rad. Both signals are then applied separately to the two electrodes of the DE-MZM. Using the recovered downstream wavelength at the input of the DE-MZM biased at quadrature, the output of the modulator produces the upstream optical signal with an OSSB+C modulation format, which is then transmitted through the network via the OADM interface.

III. Configurations for Optical Carrier Recovery

To realize the optical recovery and wavelength reuse at the BS, we propose two novel configurations, which are based on optical filtering of the downstream signal using optical FBG filters. The optical carrier recovery configuration labeled A and shown in Fig. 2 is based on an optical coupler in conjunction with an optical filter (FBG1 in the schematic). Here the incoming downstream signal is split equally by a $50:50$ optical coupler. One part of the signal is then input into a PD, which converts the signal into an electrical downstream signal. The other part of the downstream optical signal is injected into a custom designed FBG (FBG1) via an optical isolator, which prevents any reflected signals from FBG1 entering the network interface and the downstream PD. FBG1 is designed so as to have a transmission profile where transmission at the wavelength corresponding to the downstream modulation sideband is close to zero and transmission elsewhere is close to 100%. Such a transmission profile allows the downstream modulation side-

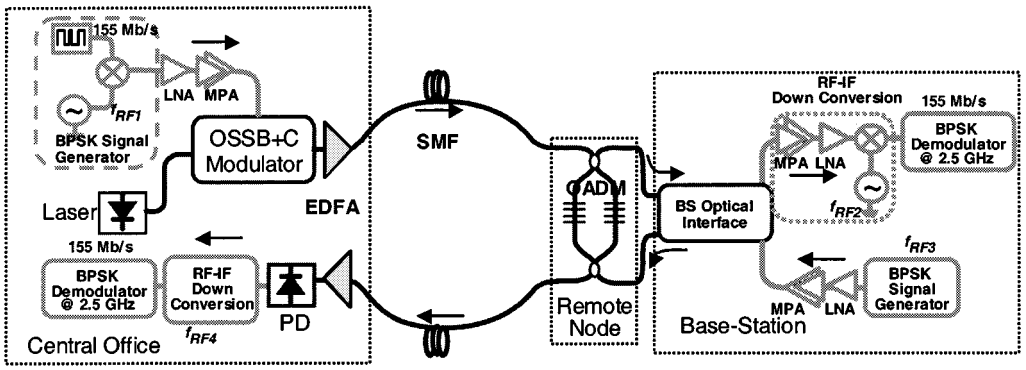

Fig. 4. Experimental setup for demonstration of the two optical carrier recovery schemes.

band to be reflected while the optical carrier is passed through the grating filter to be reused for upstream transmission.

The main advantage of the coupler approach for optical carrier recovery is that it is very simple and has the potential to be integrated onto a waveguide device if the optical isolator is used at the input to the coupler (rather than between the coupler and FBG1 as depicted in Fig. 2). The main drawback, however, of configuration A is the waste of downstream signal power, since 50% of the power in the downstream modulation sideband is also lost during the optical carrier recovery. The other drawback is that the millimeter-wave frequencies used at the BS are required to be known precisely for the design of FBG1. This leads to a lack of flexibility as any changes in frequency channel assignments will dictate a redesign or retuning of the filter if the bandwidth of the notch is not broad enough.

In order to overcome some of the limitations associated with the approach of configuration A, configuration B is proposed, which is based on an optical circulator in conjunction with an FBG filter. As shown in Fig. 3, the technique uses a custom-designed FBG (FBG2), which has a different transmission profile than that of FBG1. In configuration B, the downstream signal from the OADM interface is injected into port 1 of the optical circulator. The signal output from port 2 of the circulator is then passed through FBG2, which has 50% reflectivity at the wavelength corresponding to the downstream optical carrier and 100% reflectivity at all other wavelengths. Meanwhile, the reflected carrier (50%) is collected at port 3 of the circulator.

The output of FBG2 in Fig. 3 feeds a PD and the detected downstream signal is then fed into the BS downstream RF interface. However, the modulated upstream optical signal is fed into the OADM and transported back to the CO. If a four-port circulator is used in this approach, it will provide sufficient isolation against any backreflections reaching the network interface via port 1. The key advantage of configuration B is that no downstream signal power is wasted since only the 50% carrier component is extracted and the modulation sideband is allowed in full to reach the PD. In addition, knowledge of the operating wavelength is sufficient for the design of FBG2, making it more flexible in terms of frequency assignment at the BS–air interface.

IV. Experimental Setup

To demonstrate the simplified designs of the BS optical interface, a full duplex millimeter-wave fiber link, as shown in Fig. 4, was implemented. By multiplying a bi-polar psuedo-random signal generated by the pattern generator from a bit-error-rate (BER) test-set with a millimeter-wave local oscillator signal at a frequency of $f_{\mathrm{RF1}} = 38.0$ GHz, a BPSK formatted downstream signal is generated. The signal was then boosted in power by an amplifier chain comprising a low-noise amplifier (LNA) followed by a medium-power amplifier (MPA), before being applied to the OSSB+C modulator for generating an OSSB+C formatted downstream optical signal. A narrow-linewidth signal from a tunable laser at a wavelength of 1556.4 nm is used as the optical source. As described earlier, DE-MZM is used to generate the OSSB+C signals.

The optical signal was then boosted in power by an erbium-doped fiber amplifier (EDFA) before transmission to the BS via a 20-km standard single-mode fiber (SMF). The SMF is connected to a remote node (RN) comprising an OADM based on an interferometer in conjunction with two identical FBG filters, which have ~100% reflectivity at a wavelength assigned for the BS. The signal from the drop port then feeds the downstream fiber of the BS optical interface, the detailed construction of which is shown in Fig. 1. After detection at the BS optical interface, the electrical downstream signal is first amplified and then down-converted to an intermediate frequency (IF) of 2.5 GHz using a millimeter-wave local oscillator (LO) signal at $f_{\mathrm{RF2}} = 35.5$ GHz. The BPSK-formatted IF signal is then demodulated using a phase-locked loop (PLL) based on a Costas loop circuit. The recovered signal was then used in eye-diagram and BER measurements of system transmission quality.

In the upstream direction, a BPSK signal generator with a construction similar to that used in downstream transmission at the CO is used to generate a 155-Mb/s BPSK formatted millimeter-wave signal at the upstream transmission frequency of $f_{\mathrm{RF3}} = 34.4$ GHz. The electrical upstream signal is then amplified before being applied to the upstream OSSB+C modulator located in the BS optical interface, as shown in Fig. 1. Both configurations for optical recovery were implemented in order to verify their operation. The recovered wavelength signal was used as the optical input signal to the modulator and the output OSSB+C formatted upstream optical signal was then transmitted into the network via the add port of the OADM and transported over another 20 km of SMF before reaching the CO.

At the CO, the received optical signal is optically amplified by a low-noise EDFA before being detected by a high-speed PD. A narrow-bandwidth optical filter was used after the EDFA to

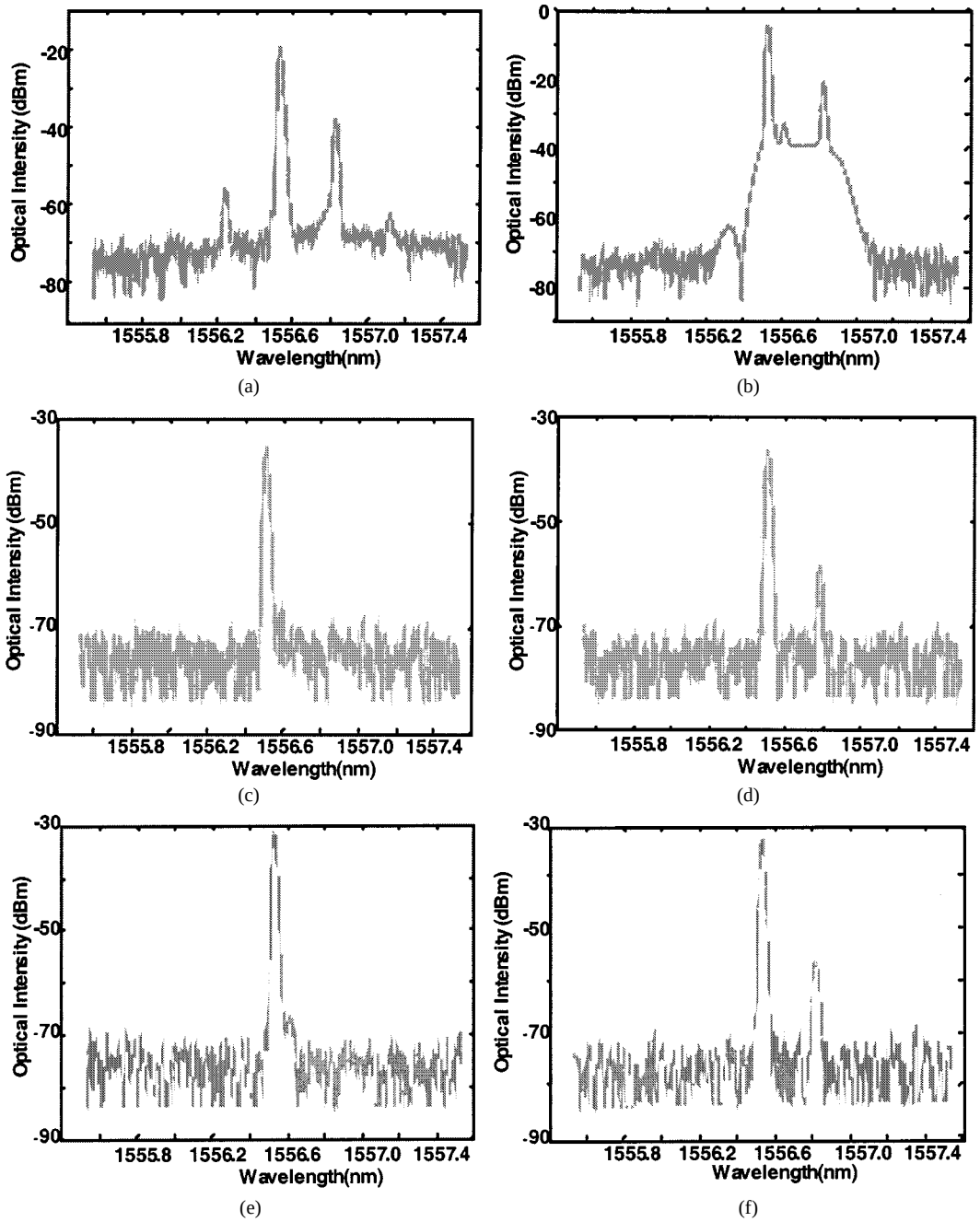

Fig. 5. Measured optical spectra at important points in the experimental setup showing optical recovery using configurations A and B. (a) Optical spectrum at the downstream optical modulator output (10% monitor). (b) Optical spectrum at the output of the OADM drop port. (c) Optical spectrum of the recovered optical carrier in configuration A. (d) Optical spectrum of the modulated upstream signal in configuration A. (e) Optical spectrum of the recovered optical carrier in configuration B. (f) Optical spectrum of the modulated upstream signal in configuration B.

reject any out-of-band amplified spontaneous emission (ASE) noise. The detected signal is then directed to a down-conversion stage where the upstream signal is down-converted to a convenient IF frequency of 2.5 GHz using an LO signal at $f_{\mathrm{RF4}} = 31.9$ GHz before being demodulated to recover the data. Finally, the recovered signal was measured and compared with that of the transmitted data.

V. Experimental Results and Discussions

Fig. 5(a) shows the measured optical spectrum of the downstream OSSB+C optical signal at the output of the modulator showing a lower sideband rejection of approximately 17 dB. This poor modulation depth is due to the bandwidth of the DE-MZM modulator (18 GHz), which was well below the downstream modulation frequency of 38.0 GHz. The amplified downstream signal after transmission over 20 km of SMF was selected by the OADM and the optical spectrum at the output of the drop port of the OADM is shown in Fig. 5(b). The suppression of the lower sideband and out-of-band ASE by the narrow-bandwidth (50 GHz) optical filters in the OADM can be clearly seen in Fig. 5(b).

When the optical carrier was recovered using configuration A [see Fig. 5(c)], the measured optical spectrum of the recovered

TABLE I
MEASURED RIN VALUES OF OPTICAL SIGNALS AT VARIOUS STAGES OF OPTICAL CARRIER RECOVERY

OPTICAL SIGNALS	MEASURED RIN VALUES
Tunable Laser Output	-138 dBc/Hz
Amplified Tunable Laser Ouput	-127 dBc/Hz
Recovered Optical Carrier using Configuration A	-125 dBc/Hz
Recovered Optical Carrier using Configuration B	-126 dBc/Hz

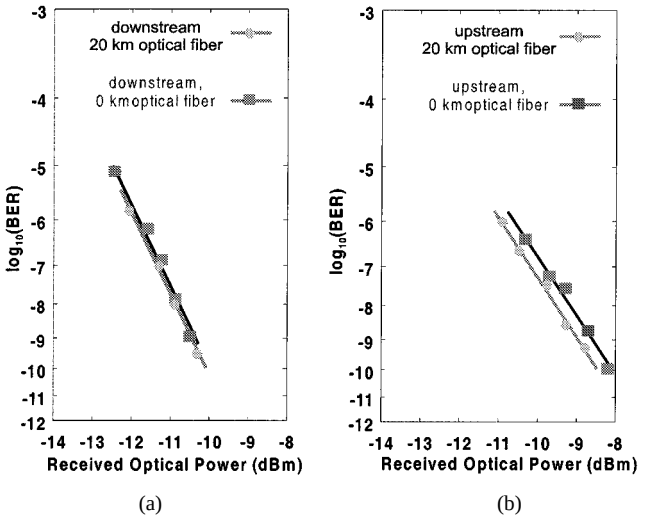

Fig. 6. Measured BER curves as function of received optical power for configuration A. (a) Downstream transmission. (b) Upstream transmission.

optical carrier at 1556.4 nm and removal of the upper sideband of the downstream signal can be clearly seen. The recovered carrier was then modulated with an upstream BPSK signal at 34.4 GHz using another OSSB+C modulator (with a similar modulation bandwidth and slightly higher insertion loss compared to the downstream modulator), and the measured optical spectrum at the output of the modulator is shown in Fig. 5(d). The modulator was biased such that it generated an OSSB+C signal with suppression of the lower modulation sideband, as shown in Fig. 5(d). Here again, the poor modulation depth seen is attributed to the low modulation bandwidth of the modulator.

Fig. 5(e) shows the measured optical spectrum of the recovered optical carrier at a wavelength of 1556.4 nm when the optical carrier was recovered using configuration B. The measured optical spectrum of the output of the modulator is shown in Fig. 5(f) showing the carrier with an upper modulation sideband.

Having demonstrated optical carrier recovery using both configurations A and B, it is also important to establish that the noise property of the recovered carrier does not degrade significantly. To investigate this, RIN measurements were performed using a lightwave spectrum analyzer (HP7000 Lightwave Analyzer) in conjunction with an RIN measurement utility (Agilent Technologies, Application Note PN71400-1). The RIN was measured for the tunable laser source used in the experiment, the amplified tunable laser signal, and the recovered carrier signals in both configurations A and B. The measured results are summarized in Table I. It can be seen that the major source of degradation is due to the impact of ASE arising from the optical amplification. In both configurations, the measured RIN of the recovered optical carrier is comparable to that of the amplified signal after transmission through 20 km of fiber, and these values are still low.

In the downstream transmission experiment, 155-Mb/s data transmission at 38.0 GHz using BPSK modulation over 20 km of SMF was carried out while the upstream transmission of a 155-Mb/s BPSK signal at 34.4 GHz over 20 km of SMF was performed simultaneously by employing optical carrier recovery using configurations A and B. Demodulation of the BPSK data was achieved with the same PLL for both down- and upstream transmission, and, therefore, BER measurements were obtained separately (not simultaneously) for upstream and downstream transmission.

Fig. 6(a) shows the measured BER results using configuration A for optical carrier recovery and for optical fiber transmission distances of 0 and 20 km in the downstream direction. For upstream data transmission using the recovered optical carrier based on configuration A, the measured BER results for 0- and 20-km upstream transmission are shown in Fig. 6(b). The negative power penalty observed between the 0- and 20-km upstream data transmission may be due to some residual chirp arising from nonequal drive signals being applied to the two electrodes of the DE-MZM used for upstream signal transmission. When configuration B was used with the transmission experiment depicted in Fig. 4, almost similar BER results to those for configuration A were obtained, as shown in Fig. 6(a) and (b). As discussed earlier, it was expected that downstream transmission with configuration B would be improved as no downstream modulation signal power is wasted. However, in the experiment, due to imperfections in the custom-designed FBG2 and due to 1-dB insertion loss of the circulator, approximately the same RF power was generated as with configuration A, leading to very similar BER results. However, with the improved fabrication of FBG2, an improvement in BER can be achieved.

The previous measurements have clearly shown the successful demonstration of both proposed techniques for optical carrier recovery. As inclusion of any optical amplification at the BS will add to the complexity of the fiber-radio system, the demonstration instead used optical amplifiers at the central office in both up- and downstream directions. In order to achieve acceptable link power budgets, however, sufficiently large optical power must be launched into the optical fiber at the CO. Since narrow-linewidth optical sources are used at the CO, stimulated Brillouin scattering (SBS) will place an upper limit on the maximum optical power that can be launched into the optical fiber. While the modulators used in the experiment had insertion losses of the order of 7.0–9.5 dB, modulators exhibiting significantly lower loss are commercially available and may ease the high launch power requirements. In addition,

if the length of transmission optical fiber is long, it may also add additional insertion loss, which may not be able to be compensated via more amplification due to the SBS limit. In systems employing the optical carrier recovery techniques described in this paper, there is a need for optimizing both the optical signal-to-noise ratio as well as the power budget, which can be achieved by using components with low insertion loss.

VI. Conclusion

We have proposed and demonstrated a simplified optical interface for an antenna BS in a millimeter-wave fiber-wireless system by incorporating two novel configurations for optical carrier recovery. Configuration A uses an optical coupler in conjunction with a custom-esigned FBG filter, which recovers part of the downstream optical carrier by removing the modulation sidebands. Configuration B recovers the optical carrier by reflecting only a part of the downstream carrier in another custom-esigned fiber Bragg grating filter in conjunction with an optical circulator. Experimental results were presented demonstrating the successful operation of both optical carrier recovery configurations. Measured RIN values of the recovered optical carriers in both configurations show that they are not degraded due to the recovery process. A full duplex 20-km optical transmission of 155-Mb/s BPSK signals using 38.0 GHz as the downstream RF frequency and 34.4 GHz as the upstream transmission frequency was carried out between the central office and the antenna BS. With both configurations, a BER of 10^{-9} was obtained. The results from our experiment indicate that such interfaces, which avoid the use of optical sources at the base stations can be realized and can greatly simplify the overall BS architecture in fiber-radio systems.

References

[1] J. R. Forrest, "Communication networks for the new millennium," *IEEE Trans. Microwave Theory Tech.*, vol. 47, pp. 2195–2201, Dec. 1999.

[2] H. Ogawa, D. Polifko, and S. Banba, "Millimeter-wave fiber-optic systems for personal radio communication," *IEEE Trans. Microwave Theory Tech.*, vol. 40, pp. 2285–2293, Dec. 1992.

[3] L. Nöel, D. Wake, D. G. Moodie, D. D. Marcenac, L. D. Westbrook, and D. Nesset, "Novel techniques for high capacity 60 GHz fiber-radio transmission systems," *IEEE Trans. Microwave Theory Tech.*, vol. 45, pp. 1416–1423, Aug. 1997.

[4] B. Mukherjee, "WDM optical communication networks: Progress and challenges," *IEEE J. Select. Areas Commun.*, vol. 18, pp. 1810–1824, Oct. 2000.

[5] G. H. Smith, D. Novak, and C. Lim, "A millimeter-wave full duplex fiber-radio star-tree architecture incorporating WDM and SCM," *IEEE Photon. Technol. Lett.*, vol. 10, pp. 1650–1652, Nov. 1998.

[6] A. Stöhr, K. Kitayama, and D. Jäger, "Error-free full-duplex optical WDM-FDM transmission using an EA transceiver," in *Proc. Int. Microwave Photon. Topical Meeting*, Princeton, NJ, 1998, pp. 37–40.

[7] H. Schmuck, "Comparison of optical millimeter-wave system concepts with regard to chromatic dispersion," *Electron. Lett.*, vol. 31, pp. 1848–1849, 1995.

[8] U. Gliese, S. Nørskov, and T. N. Nielsen, "Chromatic dispersion in fiber-optic microwave and millimeter-wave links," *IEEE Trans. Microwave Theory Tech.*, vol. 44, pp. 1716–1724, Oct. 1996.

[9] H. Schmuck, "Carrier-to-noise limitations in optical mm-wave links due to phase-induced intensity-noise," *Electron. Lett.*, vol. 33, pp. 1236–1237, 1997.

[10] G. H. Smith, D. Novak, and Z. Ahmed, "Overcoming chromatic-dispersion effects in fiber-wireless systems incorporating external modulators," *IEEE Trans. Microwave Theory Tech.*, vol. 45, pp. 1410–1415, Aug. 1997.

[11] D. Wake, D. Johansson, and D. G. Moodie, "Passive pico-cell—New in wireless network infrastructure," *Electron. Lett.*, vol. 33, pp. 404–406, 1997.

[12] L. D. Westbrook, L. Nöel, and D. G. Moodie, "Full-duplex 25 km analogue fiber transmission at 120 Mbytes/s with simultaneous modulation and detection in an electroabsorption modulator," *Electron. Lett.*, vol. 33, pp. 694–695, 1997.

[13] A. Stöhr, K. Kitayama, and D. Jäger, "Full-duplex fiber-optic RF subcarrier transmission using a dual-function modulator/photodetector," *IEEE Trans. Microwave Theory Tech.*, vol. 47, pp. 1338–1341, July 1999.

[14] A. Nirmalathas, C. Lim, D. Novak, and R. Waterhouse, "Optical interfaces without light sources for base-station designs in fiber-wireless systems incorporating WDM," in *Proc. MWP'99*, Melbourne, Australia, pp. 119–122.

[15] ——, "Optical carrier re-use in the antenna base-station of a fiber-wireless system incorporating WDM," in *Proc. OECC2000*, Chiba, Japan, pp. 442–443.

Ampalavanapillai Nirmalathas (M'97) received the B.E. (with honors) and Ph.D. degrees in electrical and electronic engineering from The University of Melbourne, Melbourne, Vic., Australia, in 1993 and 1997, respectively.

In 1997, he joined the Photonics Research Laboratory (PRL), a member of the Australian Photonics Cooperative Research Centre (CRC), University of Melbourne, where he is currently a Senior Lecturer. He is also the Research Director of the PRL and Manager of the Telecommunications Technologies Research Program at the Australian Photonics CRC. His research interests include fiber-optic feed networks for wireless systems, modeling of optical and wireless communication systems, high-speed communication technologies, and optical networks.

Dalma Novak (S'90–M'91–SM'01) received the B.E. (with first-class honors) and Ph.D. degrees in electrical engineering from the University of Queensland, Brisbane, Australia, in 1987 and 1992, respectively. Her doctoral dissertation investigated the dynamic behavior of directly modulated semiconductor lasers.

From January 1992 to August 1992, she was a Lecturer in the Department of Electrical and Computer Engineering, University of Queensland. In September 1992, she joined the Photonics Research Laboratory (PRL) [a member of the Australian Photonics Cooperative Research Centre (CRC)], Department of Electrical and Electronic Engineering, University of Melbourne, Melbourne, Australia, where she is currently an Associate Professor and Reader. Her responsibilities have included Deputy Director and Research Director of the PRL, CRC Key Researcher, Director of the CRC Melbourne Division, and CRC Education Director. From December 1999 to March 2001, she was a Director of Australian Photonics Pty Ltd. In July–October 2000 and October 2000–January 2001, she was a Visiting Researcher in the Department of Electrical Engineering, University of California at Los Angeles (UCLA) and the Naval Research Laboratory, Washington, DC. In June 2001, she joined Dorsál Networks Inc., Columbia, MD. Her research interests include fiber-radio communication systems and high-speed opto-electronic devices and circuits. She has authored or co-authored over 150 papers in these areas.

Dr. Novak is a member of the Microwave Photonics Technical Subcommittee of the IEEE Lasers and Electro-Optics Society (IEEE LEOS) and was chair of the IEEE LEOS Victorian Chapter from 1998 to 2001. She is a former chair of the International Topical Meeting on Microwave Photonics (MWP) Steering Committee and was general co-chair of MWP'99, Melbourne, Australia, November 1999.

Christina Lim (S'97–M'00) received the B.E. (with first-class honorss) and Ph.D. degrees in electrical and electronic engineering from The University of Melbourne, Melbourne, Vic., Australia, in 1995 and 2000, respectively.

Since November 1999, she has been a Research Fellow with the Fiber-Radio Group, Photonics Research Laboratory (PRL), University of Melbourne. Her research interests include fiber-optic wireless communication systems, applications of mode-locked lasers, and optical communication systems.

Rodney B. Waterhouse (S'90–M'92) received the B.E. (with honors), M.Eng.Sc. (research), and Ph.D. degrees from the University of Queensland, Brisbane, Australia, in 1987, 1990, and 1994, respectively.

In 1994, he joined the Department of Communication and Electronic Engineering, RMIT University [a member of the Australian Photonics Cooperative Research Centre (CRC)], Melbourne, Vic., Australia, where he is currently a Senior Lecturer. He is also a Key Researcher at the Australian Photonics CRC. His research interests include printed antennas, phased arrays, optically distributed wireless systems, and photonic devices for microwave applications. He has authored or co-authored over 120 papers in these areas.